International Journal of Modern Physics: Conference Series

EXCLUSIVE MEASUREMENTS OF OMEGA ELECTROPRODUCTION OFF THE PROTON IN THE RESONANCE REGION

EVAN PHELPS (for the CLAS Collaboration)
Department of Physics and Astronomy, University of South Carolina
Columbia, South Carolina 29208, USA
ephelps@jlab.org

Received 10 August 2013

A complete theory of strong interactions must describe the excited baryon spectrum as well as the structure of each excited state, which extends into the virtual photon domain and reflects the dynamics of nonperturbative QCD. The experimental challenge of extracting the prerequisite Q^2-dependent information is complicated by multi-channel couplings and overlapping excited states. Beyond the discriminating power of exclusive single- and double-pion electroproduction, the $\omega\,(783)$ channel provides an excellent probe of excited states in the third resonance region. The current analysis provides preliminary differential and integrated cross-sections of ω electroproduction off the proton from $W = 1.7$ to $3.2\,\mathrm{GeV}$ and $Q^2 = 1.5$ to $5.5\,\mathrm{GeV}^2$. The data was collected by JLab's CLAS detector during two run periods and comprises the largest sample of exclusive resonance-region ω electroproduction ever analyzed. Preliminary Legendre decomposition of the cross-sections supports previous indications of s-channel contributions to cross-sections in the resonance region.

Keywords: electroproduction; vector meson production; ω production.

PACS numbers: 25.30.Rw, 13.60.Le

1. Introduction

The QCD Lagrangian might contain the full story of strong interactions, but it does not directly provide much insight into some of its own most important features emerging in the nonperturbative regime.[1] The information needed to explore these dynamical features is encoded in the baryon spectrum and elastic and transition form factors. Photoproduction experiments serve as excellent probes of the excited baryon spectrum, while electroproduction experiments afford access to form factors that extend our view of the baryons into the virtual photon domain.

The experimental challenges of accessing this information[2,3] are mitigated by exclusive measurements and selective production channels, such as $\gamma_v p \to \omega p$, which is highly discriminating in several ways: First, the majority of world data is derived from π production. ω might couple to previously undetected resonances more strongly than π. Second, the isoscalar nature of ω restricts its couplings to isospin-

1/2 resonances. Finally, the narrow 9-MeV ω decay width reduces systematic errors introduced during background subtraction. In this analysis, exclusive ω production off the proton is studied via the three-pion decay channel,

$$\gamma_v p \to \omega p \to \pi^+\pi^-\pi^0 p\,.$$

The ω production is described in terms of four independent variables, W, Q^2, $cos\,\theta^*$, and ϕ^*, where θ^* and ϕ^* are the polar and azimuthal angles of the ω three-momentum in the right-handed, center-of-momentum coordinate system with $\hat{u}_y = \hat{u}_e \times \hat{u}_{e'}$ normal to the electron scattering plane.

Under the one-photon-exchange assumption, the scattering matrix factorizes into the well-known leptonic part and the unknown hadronic part. The corresponding differential cross-section is expressed as

$$\frac{d^4\sigma}{dW dQ^2 d\Omega^*} = \Gamma \frac{d^2\sigma_h}{d\Omega^*}\,, \tag{1}$$

where $\Gamma = \Gamma(W, Q^2)$ is the virtual photon flux that normalizes events according to the probability density of producing a virtual photon. The resulting hadronic cross-sections are decomposed into the unpolarized cross-section $\sigma = \sigma_T + \epsilon\sigma_L$ and the interference terms σ_{TT} and σ_{LT} according to the virtual photon polarization, ϵ:

$$\frac{d^2\sigma_h}{d\Omega^*} = \sigma_T + \epsilon\,\sigma_L + \epsilon\,\sigma_{TT}\,cos(2\phi^*) + \sqrt{2\epsilon(1+\epsilon)}\,\sigma_{LT}\,cos(\phi^*)\,. \tag{2}$$

Connecting the hadronic cross-sections to the binned experimental data yields

$$\frac{d^2\sigma_h}{d\Omega^*} \simeq \frac{1}{BL\,\langle\Gamma\rangle\,\Delta W \Delta Q^2} \cdot \frac{1}{\prod_i w^i} \cdot \frac{N}{\Delta\Omega^*}\,, \tag{3}$$

where $B = 0.891$ is the branching ratio for ω's three-pion decay[4]; L is the integrated luminosity; ΔW, ΔQ^2, and $\Delta\Omega^*$ multiply to give the four-dimensional bin volume; each w^i is a correction factor (Section 2 lists corrections); and N is the yield in one bin of the four-dimensional kinematic space.

2. Experimental setup and data reduction

The current work analyzes data collected with the CLAS detector[5] during E1F and E1-6 run periods. Unpolarized liquid Hydrogen targets were subjected to 5.5- (E1F) and 5.8-GeV (E1-6) longitudinally polarized electrons from JLab's continuous electron beam. The integrated luminosity is 21 fb^{-1} for E1F and 28.5 fb^{-1} for E1-6. Both run periods utilized reduced magnetic fields to enhance detection of inward-bending negative pions that would otherwise pass through the forward hole of the CLAS detector. Data acquisition was triggered by conincident and geometrically consistent hits in the Čerenkov detector (CC) and forward electromagnetic calorimeter (EC), permitting electrons above 0.5 GeV

The ω kinematics can be determined from the reconstructed electron and proton, but to enhance the signal to background ratio, detection of at least one of its decay

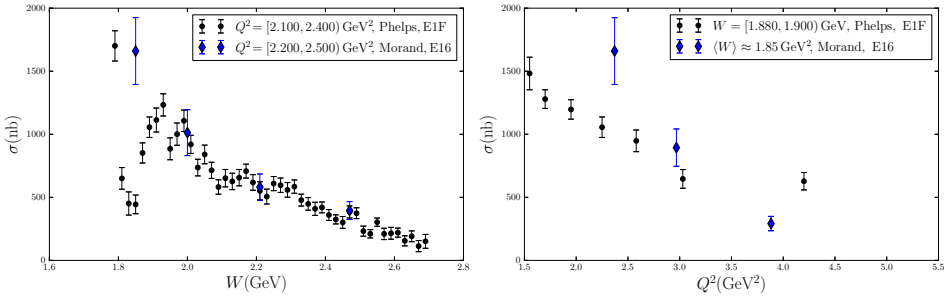

Fig. 1. Unpolarized cross-sections in sample Q^2 (left) and W (right) with legend indicating sources. Preliminary E1F results are from partial statistics with statistical error bars only. The published E1-6 results (Ref. 6) are transformed from Bjorken x_b to W, so the points correspond to mean W values rather than W bins.

pions is demanded. Neutral pions are not reconstructed, so candidate events fall into three independent sets according to which particles, exclusively, were detected. These sets correspond to the following detection topologies:

$$\begin{aligned} \gamma_v p &\to p\pi^+ X \\ \gamma_v p &\to p\pi^- X \\ \gamma_v p &\to p\pi^+\pi^- X\,, \end{aligned} \tag{4}$$

where X represents all undetected particles in the event.

Surviving events are subjected to (a) electron momentum corrections, (b) hadron energy loss corrections, (c) fiducial volume cuts, (d) vertex corrections, (e) target volume cuts, and (f) CC cuts and corrections, independent of topology.

Topology-dependent cuts and corrections include (g) two-dimensional missing-mass event selection on MM_p versus $MM_{p\pi^+}$, $MM_{p\pi^-}$, or $MM_{p\pi^+\pi^-}$, (h) side-band background subtraction in four-dimensional kinematics, and (i) simulation-determined acceptance, efficiency, and radiative corrections.

3. Preliminary results

Preliminary results presented here derive from the $\gamma_v p \to p\pi^+ X$ detection topology of E1F. With these partial statistics, $\sigma_T + \epsilon\sigma_L$ is extracted (see, e.g., Figure 1 with comparison points from Ref. 6 denoted) and decomposed into Legendre moments $l \leq 2$ and t-/u-channel contributions according to ϕ-integrated differential cross-sections in 20-MeV W bins and variable-width Q^2 bins,[a] as illustrated by sample fits in Figure 2. The representative fits serve to communicate some important features revealed by this analysis, especially with respect to the W and Q^2 evolution of s- and t-channel contributions: At low W, exemplified by $W = 1.79\,\text{GeV}$ in column 1, σ is

[a]Interference terms (not shown here) are decomposed according to the fully differential cross-sections with the same W, Q^2, and $\cos\theta^*$ binning and an additional dimension of 19 ϕ^* bins.

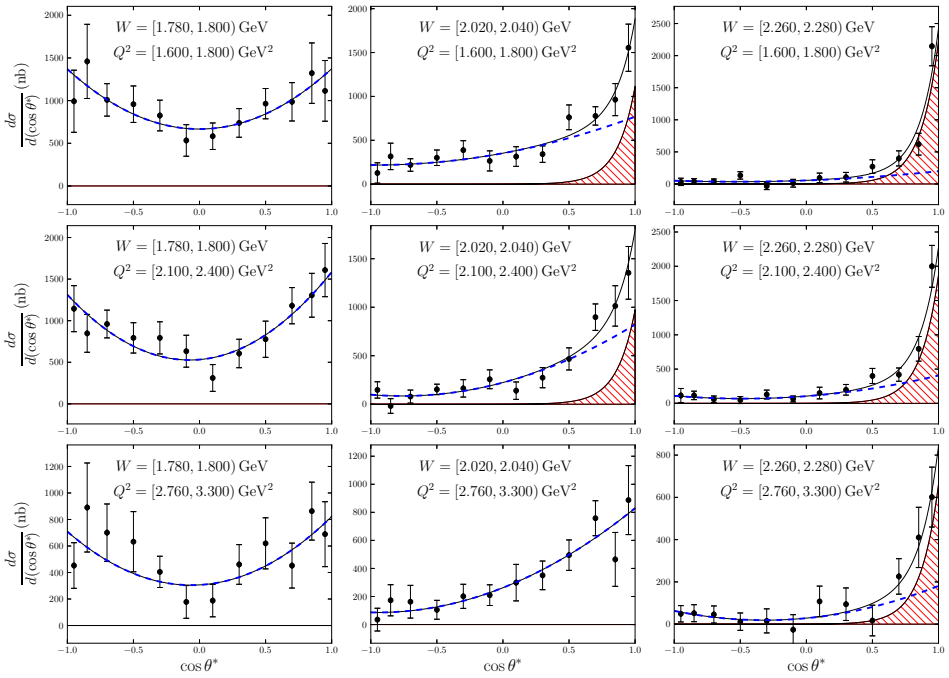

Fig. 2. ϕ-integrated differential cross-sections in sample W, Q^2 bins. Solid black curves represent total fits; dotted blue curves represent Legendre contributions, limited to $l \leq 2$; red filled regions represent t-channel contributions. u-channel contributions are not required in the selected bins.

describable by $l \leq 2$ Legendre polynomials alone. For $W > 1.9\,\text{GeV}$, as in columns 2 and 3, t-channel contributions enhance the forward angle cross-sections but diminish with increasing Q^2 more quickly than s-channel Legendre contributions. For $W > 2.3\,\text{GeV}$, the t channel dominates with increasing relative strength, as expected.

4. Acknowledgements

This work is supported in part by the National Science Foundation, Grant No. 0856010, and the Jefferson Science Associates Graduate Fellowship Program.

References

1. N. Isgur, Why N*'s are important, in *Excited Nucleons and Hadronic Structure*, NStar 2000, Newport News, VA, eds. V. D. Burkert, L. Elonadrihiri, and J. J. Kelly (World Scientific, Singapore, 2001), p. 403.
2. R. W. Gothe, AIP Conf. Proc. **1432**, 26 (2012) [arXiv:1108.4703 [nucl-ex]].
3. I. Aznauryan, et al., Int.J.Mod.Phys. E22, 1330015 (2013), 1212.4891.
4. J.Beringer et al. (Particle Data Group), Phys. Rev. D86, 010001 (2012).
5. B.A. Mecking et al., NIM A503, 513-553 (2003).
6. L. Morand *et al.* Eur. Phys. J. A **24**, 445 (2005) [hep-ex/0504057].